CHEMISTRY
A EUROPEAN JOURNAL

FULL PAPER

DOI: 10.1002/chem.201201437

Synthesis and Characterization of Reversible Chemosensory Polymers: Modulation of Sensitivity through the Attachment of Novel Imidazole Pendants

Rudrakanta Satapathy, Harihara Padhy, Yen-Hsing Wu, and Hong-Cheu Lin*[a]

Abstract: Three novel electron donor–acceptor conjugated polymers (**P1**–**P3**) bearing various imidazole pendants have been synthesized. Their excellent photophysical and electrochemical properties make them suitable transduction materials for chemosensing applications. Indeed, polymers **P1**–**P3** have been found to show remarkable sensing capabilities towards H^+ and Fe^{2+} in semi-aqueous solutions. Upon titration with H^+, polymers **P1** and **P2** showed hypsochromic shifts of their absorptions and photoluminescence (PL) maxima with enhanced fluorescence intensities. However, **P3** showed diminished absorption and fluorescence intensities under similar conditions due to static quenching. The anomalous behavior of **P3** compared with **P1** and **P2** has been clarified in terms of electronic distributions through computational analysis. Furthermore, **P3** ($K_{SV}=1.03\times10^7$) showed a superior sensing ability towards Fe^{2+} compared with **P1** ($K_{SV}=2.01\times10^6$) and **P2** ($K_{SV}=4.12\times10^6$) due to its improved molecular wire effect. Correspondingly, the fluorescence lifetime of **P3** was greatly decreased (almost 11-fold) compared to those of polymers **P1** (4.6-fold) and **P2** (6.2-fold) in the presence of Fe^{2+}. By means of a fluorescence on-off-on approach, chemosensing reversibilities in protonation–deprotonation and metallation–demetallation have been achieved by employing triethylamine (TEA) and the disodium salt of ethylenediaminetetraacetic acid (Na_2-EDTA)/phenanthroline, respectively, as suitable counter ligands. ^{1}H NMR titrations have revealed the unique behavior of **P3** compared with **P1** and **P2**. To the best of our knowledge, there have been no previous reports of Fe^{2+} sensors based on single imidazole receptors conjugated to a main-chain polymer showing such a diverse sensitivity pattern depending on their attached substituents.

Keywords: computational analysis · donor–acceptor systems · fluorescence · molecular wire effect · sensors · transduction material

Introduction

The molecular design of new sensors is of prime importance because of tremendous demands in analytical, biomedical, biotechnological, and nanotechnological applications.[1] The success of fluorescence-based sensors can be attributed to their advantageous features of specific sensitivity, selectivity, and real-time screening for various moieties.[2] Rigid and ladder-type low band-gap conjugated polymers can display excellent redox and optoelectronic properties, such as broad and long-wavelength light absorption, good luminescence intensity, and favorable carrier mobility, which result in potential applications in optoelectronics, microelectronics, light-emitting diodes, photovoltaics, and field-effect transistors.[3] Some interesting recent extensions of these materials concerned their subsequent application in fluorescent and biological sensors.[4] Conjugated polymers (as molecular wires) have enormous advantages over small molecules for sensing applications due to facile exciton transport and energy migration along their conjugated polymer backbones, which enhance the electronic communication between receptors and polymers.[4] Conjugated polymers are attractive for serving as semi-conductive "molecular wires" owing to their π-electron resonances through conjugations between donor–acceptor repeat units. This allows such polymers to be utilized as one of the most vital classes of sensing materials by virtue of their high sensitivities derived from molecular wire effects.[5] Furthermore, conjugated polymer sensors hold great promise because their emission intensities, absorbances, charge-transport properties, conductivities, and exciton migrations can be easily perturbed by external chemical species, such as acids, bases, and ions, leading to substantial changes in their measurable signals.[1,6,7] The incorporation of sensitive and selective functionalities (as probes) for both protons and metal ions, together with well-known fluorophores, into conjugated polymers has yielded new materials suitable for chemosensory applications.[6] Thus, the synthesis of soluble and stable fluorescent conjugated polymers has yielded improved selective recognition and transduction materials for chemical and biological sensing purposes.[8–10] A key feature for such sensing applications is a need for reversibility within certain ranges of recognition processes.[7] Imi-

[a] R. Satapathy, Dr. H. Padhy, Y.-H. Wu, Prof. H.-C. Lin
Department of Materials Science and Engineering
National Chiao Tung University
Hsinchu, R.O.C. (Taiwan)
Fax: (+886)35724727
E-mail: linhc@mail.nctu.edu.tw

Supporting information for this article is available on the WWW under http://dx.doi.org/10.1002/chem.201201437.

dazole-based ligands are widely used by virtue of their reversible fluorescence (on-off-on) by protonation/deprotonation with an acid/base as well as metallation/demetallation in the presence of metal ions/suitable counter ligands, which can induce a large energy perturbation.[6]

Fe^{2+} is the most abundant transition metal ion in biological systems and plays significant roles in metabolic processes.[7] Fe^{2+} ions are essential for most organisms, but both deficiency and overload of Fe^{2+} can cause various syndromes as a result of the disruption of iron transport, storage, and balance.[8] For example, Fe^{2+} deficiency leads to anaemia and breathing problems, while excess iron in the body causes DNA, liver, and kidney damage (hemochromatosis).[9] Introduction of specific probes, such as epoxy, bipyridine, terpyridine, quinoline, dipyrrolylquinoxaline, imidazole, and sulfate on the backbones or side chains of conjugated polymers has been successfully employed for metal ion detection on the basis of characteristic metal-to-ligand charge-transfer effects.[10] However, to the best of our knowledge, there have been no reports of Fe^{2+} sensors with a single imidazole receptor conjugated to a main-chain polymer backbone. Herein, we report three imidazole-based polymers that show remarkable sensing capabilities towards Fe^{2+}.

On the other hand, fluoride anion is of particular interest among halide anions owing to its association with preventing dental caries, as well as treatments for osteoporosis, anaesthetics, hypnotics, psychiatric drugs, and nerve gases. Its detection is also pertinent to the analysis of drinking water and the refinement of uranium used in nuclear weapon manufacture.[12a–d] The detection of fluoride is often subject to interference from other halides.[12e,f] Hence, selective fluoride detection in the presence of other halides has also become an objective of many researchers.[12g–j]

With these concepts in mind, we have synthesized three novel imidazole-based conjugated fluorescent polymers (**P1**–**P3**; Scheme 1). The photophysical and electrochemical properties of these polymers indicate that they might serve as excellent energy-transfer materials with remarkable stabilities, making them suitable for use in chemosensors. Compared with **P1** and **P2**, polymer **P3** showed a different spectral change upon pH sensing, probably due to its distinct electronic distribution. All of the polymers showed reversibility in pH sensing upon the addition of TFA as a protonating agent and TEA as a counter ligand for deprotonation. Furthermore, the quenched fluorescences of polymers **P1**–**P3** were restored upon the addition of counter ligands. Hence, reversible sensing capabilities of polymers **P1**–**P3** to-

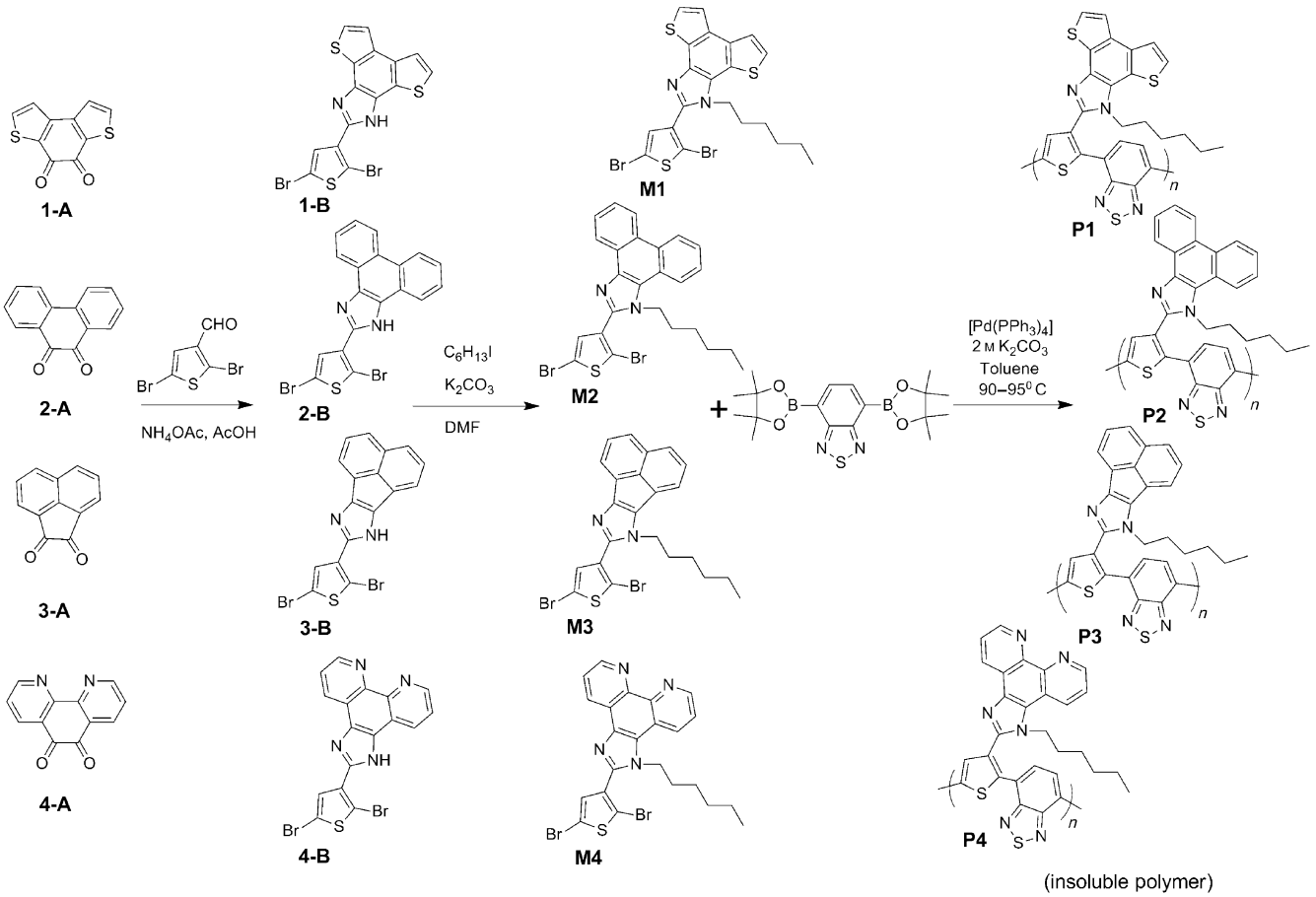

Scheme 1. Synthetic routes for the preparation of monomers and polymers.

wards Fe^{2+} ions were achieved by the addition of suitable counter ligands (Na_2-EDTA/phenanthroline). Furthermore, all of the monomeric precursors (**1B–4B**) showed distinct sensitivities towards fluoride ions over the other halides.

Results and Discussion

Synthesis: Four imidazole-based monomers (**M1–M4**) were synthesized according to Scheme 1. Benzo[1,2-*b*:4,3-*b*′]dithiophene-4,5-quinine (**1-A**) was prepared in two steps, that is, initial preparation of 3,3′-bithiophene followed by acylation with oxalyl chloride in the absence of a Lewis acid. It was found that the best route to 3,3′-bithiophene was to treat 3-bromothiophene with *n*BuLi and then to perform an oxidative coupling using commercial grade $CuCl_2$, which gave the product in 77.9% yield (Scheme S1 in the Supporting Information). Furthermore, 1,10-phenanthroline-5,6-dione (**4-A**) was prepared by treating 1,10-phenanthroline with H_2SO_4, HNO_3, and KBr.[13a] Phenanthrene-9,10-dione (**2-A**) and acenaphthylene-1,2-dione (**3-A**) were obtained from commercial sources. Imidazole derivatives (**1-B–4-B**) were obtained by cyclization of 3-thiophenecarboxaldehyde with the corresponding diketo compounds (**1-A–4-A**) using NH_4OAc in acetic acid. All imidazole derivatives (**1-B–4-B**) were directly employed without further purification. Monomers (**M1–M4**) were prepared by N-alkylation of **1-B–4-B** using K_2CO_3 as base and an alkyl iodide in DMF and were subsequently purified by column chromatography to afford good yields. To the best of our knowledge, none of these monomers has been synthesized previously. Finally, Suzuki polymerization of monomers **M1–M4** with the diboronic ester of benzothiadiazole afforded the respective polymers **P1–P4** (Scheme 1). It is worthy of mention that, except for **P4**, all of these polymers proved to be soluble in common organic solvents, such as CH_2Cl_2, $CHCl_3$, THF, and 1,2-dichlorobenzene. However, the average molecular weight of polymer **P3** (Mw = 13718) was higher than those of **P1** (Mw = 4614) and **P2** (Mw = 5755) due to the good solubility of the acenaphthylene-imidazole units in **P3** compared to the benzodithiophene units in **P1** and the phenanthrene units in **P2**. Further characterizations of polymers **P1–P3** were carried out in semi-aqueous solutions of THF/H_2O (1:1).

Photophysical characterization: Normalized absorption and emission spectra of the polymers in both solutions and solid films are shown in Figure 1, and their characteristic optical data are summarized in Table 1. All of these polymers exhibited two distinct broad absorption peaks, with the high-energy sharp peaks at 300–400 nm being attributable to d-d* transitions, and the low-energy broad bands at 500–650 nm being attributable to localized intramolecular charge trans-

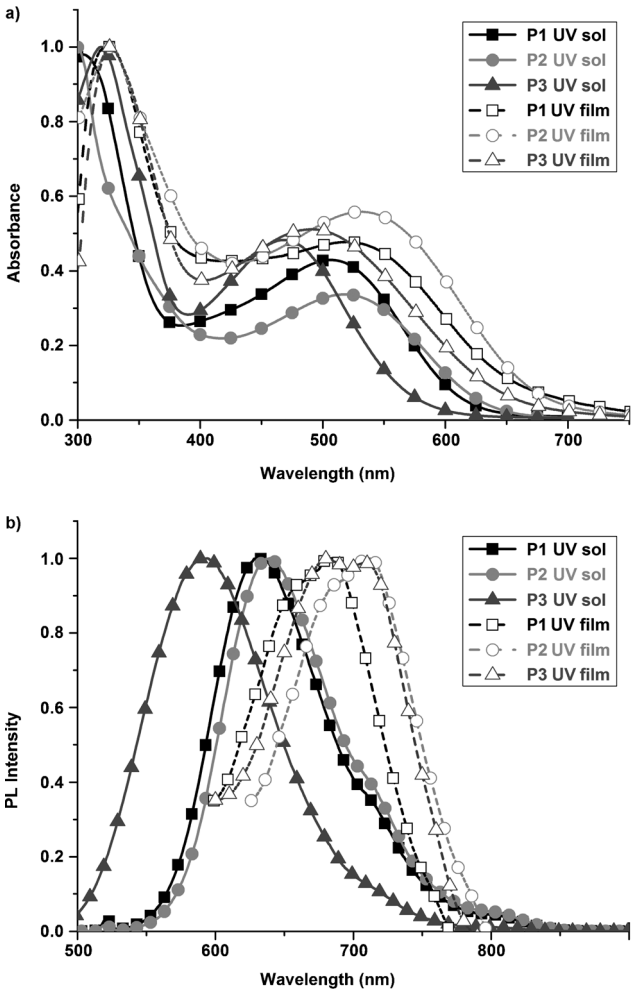

Figure 1. Normalized (a) UV absorption and (b) photoluminescence spectra of **P1**, **P2**, and **P3** in THF solutions (sol) and solid films (film).

Table 1. Photophysical, electrochemical, and thermal properties of **P1**, **P2**, and **P3.**

Polymer	Solution[a]			Film[b]			Energy levels				
	$\varepsilon_{max,abs}$ (nm)	$\varepsilon_{max,em}$ (nm)	Stokes shift[g] (nm)	$\varepsilon_{max,abs}$ (nm)	$\varepsilon_{max,em}$ (nm)	Stokes shift[g] (nm)	$\varepsilon_{onset,abs}$ (nm)	$E_{g,opt}$[e] (eV)	$E_{onset,ox}$[d] (V)/ HOMO (eV)	$E_{onset,red}$[d] (V)/ LUMO (eV)	$E_{g,el}$[f] (eV)	T_g (°C)
P1	305, 515	631	119	325, 535	(659)[c], 684	149	664	1.86	1.05/−5.40	−0.86/−3.49	1.91	234
P2	301, 521	640	119	329, 539	(684)[c], 711	172	676	1.83	1.02/−5.37	−0.87/−3.48	1.89	274
P3	319, 470	594	224	327, 497	(683)[c], 709	212	662	1.87	1.06/−5.41	−0.86/−3.49	1.92	249

[a] In THF solutions. [b] Spin-coated from THF solutions on a glass surface. [c] Shoulder peak. [d] $E_{HOMO}/E_{LUMO} = [-(E_{onset} - E_{onset\ (Fc/Fc^+\ vs\ Ag/Ag^+)}) - 4.8]$. [e] Optical bandgap $E_{g,op} = 1240/\lambda_{edge}$. [f] Electrochemical bandgap $E_{g,el} = E_{onset/ox} - E_{onset/red}$. [g] Stokes shift $= \lambda_{em} - \lambda_{abs}$.

fers between electron donors and acceptors in the polymer backbones. Significant bathochromic shifts of the absorptions as well as photoluminescence (PL) emissions of all of the polymers in solid films could be ascribed to interchain aggregations of rigid planar segments in the polymer backbones.[14a–c] The shoulders seen in the PL spectra in Figure S1(b) may be ascribed to the increased vibronic coupling associated with molecular rigidity in solid films. The noticeably larger values of the Stokes shifts of all of the polymers signify differences in the geometrical structures in the ground and excited states. This further indicates the occurrence of significant excited-state intermolecular charge transfer in the chromophores, which is essential for chemosensory applications.[14d,e] The optical bandgaps (~1.85 eV) of these polymers (**P1**–**P3**) were found to be smaller than that of P3HT (~1.90 eV)[14g] due to the combination of electron donor and acceptor moieties. In addition, the bandgaps of **P1**–**P3** were also smaller than that of the analogous polymer PT2BT (1.97 eV) containing bithiophene (as donor) and benzothiadiazole (as acceptor) units,[14h] which implies that, compared to the bithiophene unit in PT2BT, the 3-thiophene-imidazole unit (with a stronger electron-donating ability) induced more effective conjugation between the donor and acceptor segments in polymers **P1**–**P3**. Therefore, it could be concluded that polymers **P1**–**P3** have good electronic communication between receptors in their backbones through facile migration of excitons during the sensing process.[14i]

Electrochemical characterization: Cyclic voltammograms of the polymers in solid films are shown in Figure 2, and the related data are summarized in Table 1. All of the polymers displayed reversible or quasi-reversible n-doping/dedoping (reduction/reoxidation) processes at negative potentials, which indicated good structural stability in their charged states. Furthermore, the highest occupied molecular orbital (HOMO) levels of polymers **P1**–**P3** (ca. −5.4 eV) were lower than −5.2 eV, which showed their good air stability.[15c] Besides structural stability, these low HOMO levels suggest that polymers **P1**–**P3** should be capable of serving as good electron-donor materials for sensing applications.[15]

pH sensing and reversibility: The pH-sensing properties of these polymers were investigated by UV/Vis and PL titrations. As shown in Figure 3(a), upon increasing [H^+] by the addition of trifluoroacetic acid (TFA), a hypsochromic shift in the absorption maximum as well as the onset occurred, with a concomitant decrease in the absorption intensity of **P1**. Polymer **P2** showed a similar pH-sensing response (Figure 3(b)), probably due to a similar electronic distribution. At higher [H^+], the imidazole units were protonated, which hindered the effective charge transfer from the benzodithiophene and phenanthrene units to the backbones of **P1** and **P2**, respectively. The excited state was more strongly destabilized than the ground state, due to the protonation of donor imidazole units, and thus hypsochromic shifts of the absorption and emission spectra were observed.[16a] The PL

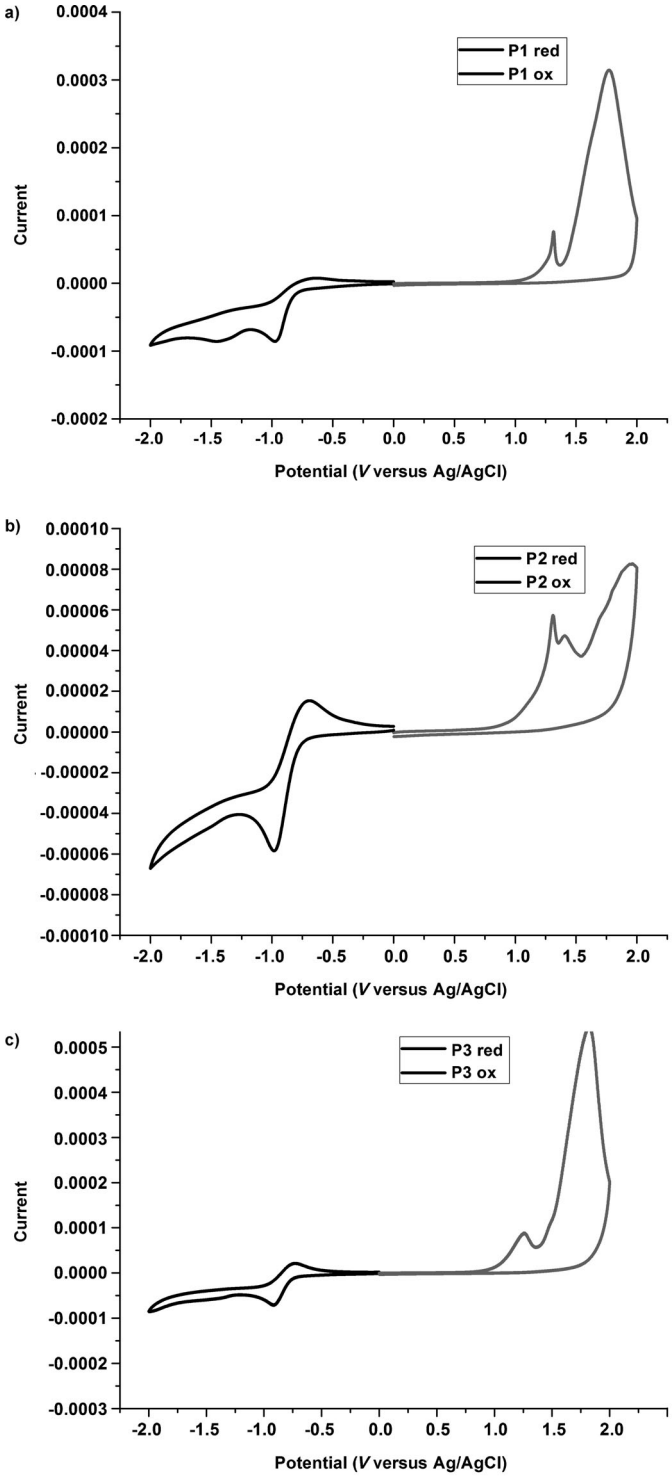

Figure 2. Cyclic voltammograms of polymers (a) **P1**, (b) **P2**, and (c) **P3** in solid films obtained at a scan rate of 100 mV s^{-1}.

spectra of **P1** and **P2** in Figure 4(a) and (b), respectively, show significant blue shifts with enhanced intensities upon increasing [H^+]. Photoinduced electron transport (PET)[16b] from the imidazole units to the polymer backbones of **P1** and **P2** caused weak fluorescence. However, protonation of

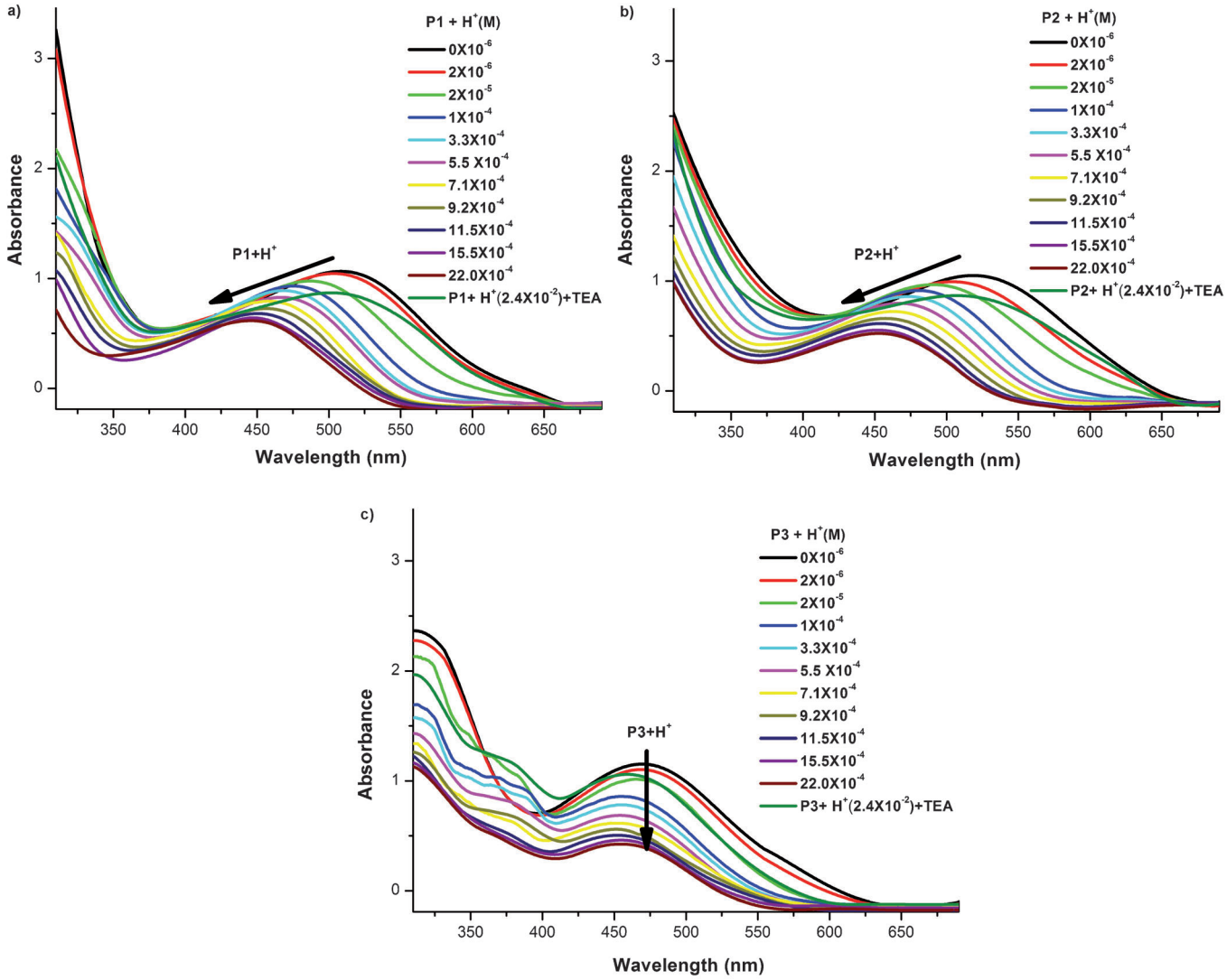

Figure 3. UV/Vis absorption spectra of (a) **P1**, (b) **P2**, and (c) **P3** in THF/H_2O (1:1) (1.4×10^{-5} M) at various concentrations of trifluoroacetic acid (TFA) and after final neutralizations with triethylamine (TEA).

the imidazole moieties diminished PET effects at higher $[H^+]$, which in turn restored the fluorescence originating from the imidazole unit and hence the fluorescence was enhanced.[16c,d] Due to the different electronic distribution of the five-membered anti-aromatic (acenaphthylene) rings in **P3**, this polymer showed a different pH response from **P1** and **P2** containing six-membered aromatic rings (benzodithiophene and phenanthrene, respectively). In contrast to **P1** and **P2**, upon increasing $[H^+]$, the absorption intensity of **P3** (Figure 3(c)) decreased without significant blue shifts of its absorption maxima. Sequentially, a new shoulder appeared at 360–400 nm at moderate $[H^+]$ ($2\times10^{-6}-2.1\times10^{-3}$ M). Surprisingly, unlike for **P1** and **P2**, the fluorescence intensities of **P3** decreased with increasing $[H^+]$ (Figure 4(c)), which could possibly be attributed to static quenching.[16e–g] The notion of static quenching was further confirmed by a Stern–Volmer plot for the fluorescence quenching of **P3** upon titration with $[H^+]$ at various temperatures (Figure 4(d)), which revealed that the binding constant of the quencher H^+ for **P3** was reduced upon increasing the temperature. Furthermore, each of the polymers recovered most of its original absorption and fluorescence upon the addition of triethylamine (TEA) due to deprotonation of the imidazolium salt. Consequently, the modulation of both the UV/Vis and PL spectra upon the addition of TFA and TEA clearly indicates that all of the polymers (**P1**–**P3**) are promising reversible pH-sensing materials in terms of both absorption and fluorescence ratiometries.

We further investigated the sensing mechanism by theoretical calculations based on computational analysis (see Figure 5). The HOMO electron clouds are mostly localized over the benzodithiophene units of **P1**, while the LUMO electron clouds are localized over the benzothiadiazole units. A more electron-rich center is induced by the aroma-

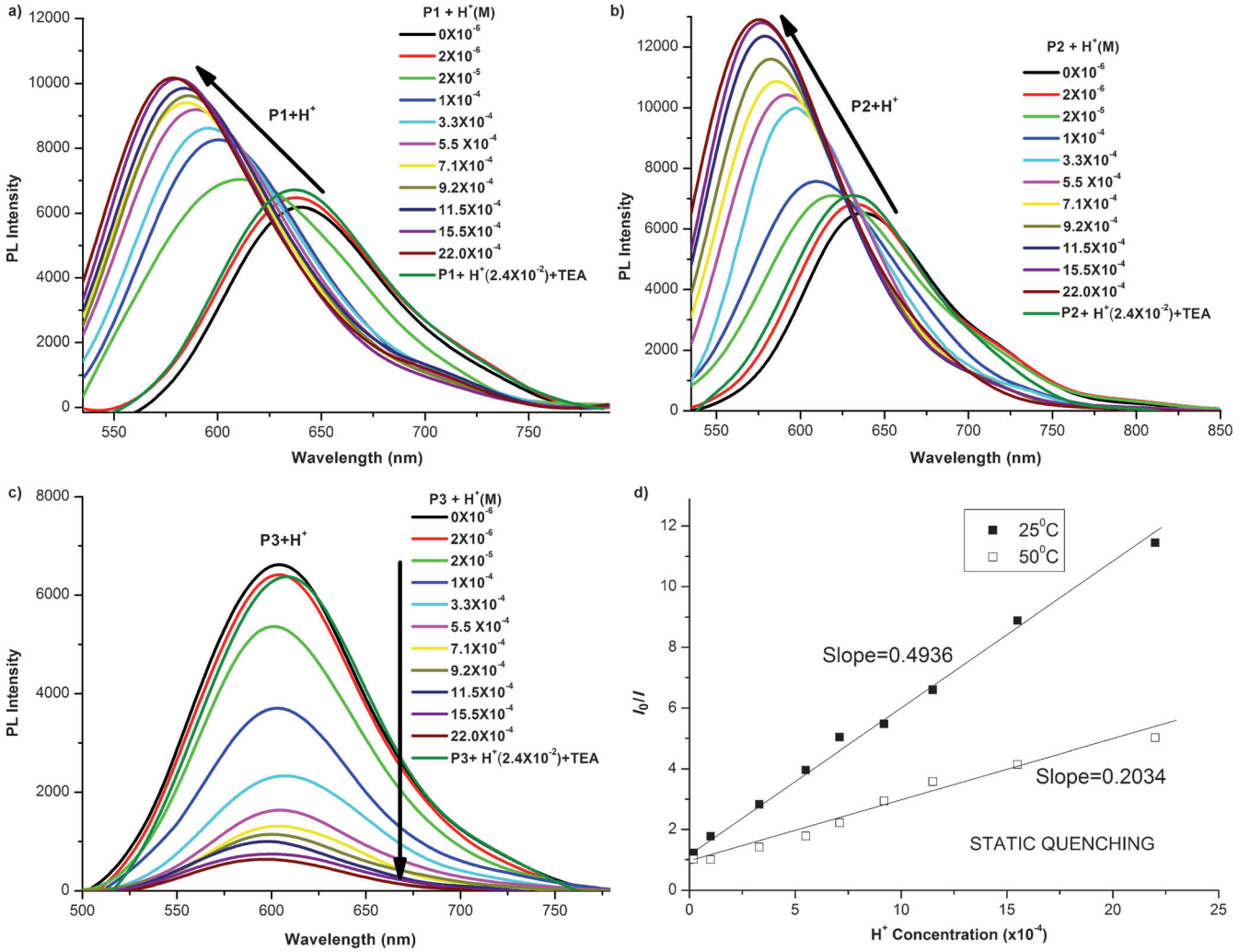

Figure 4. PL spectra of (a) **P1**, (b) **P2**, and (c) **P3** in THF/H_2O (1:1) (1.4×10^{-5} M) at various concentrations of trifluoroacetic acid (TFA) and after final neutralizations with triethylamine (TEA). Insets in (a)–(c) are the respective Stern–Volmer plots. (d) Stern–Volmer plots for the fluorescence quenching of **P3** by H^+ at 25 °C and 50 °C.

ticity of the benzodithiophene unit in **P1**, and thus the HOMO electron cloud resides over this unit. As a highly electron-accepting group, the benzothiadiazole unit gathers most of the LUMO electron cloud. Thus, there is effective intramolecular charge transfer (ICT) from the pendant benzodithiophene unit to the polymer backbone through the imidazole linkage. The aromaticity of the phenanthrene ring in **P2** makes it a strong electron-donating unit. The HOMO electron cloud is thus mostly localized over the phenanthrene unit. Similarly to **P1**, the LUMO electron cloud in **P2** is mostly localized over the benzothiadiazole unit. Thus, there is effective ICT in the polymer backbone of **P2** due to the charge-separated states. In both **P1** and **P2**, the nitrogen lone pairs of the imidazole units belong to the HOMOs of the respective polymers. Upon titration with H^+, the nitrogen lone pairs become coordinated with the H^+ ions, leading to bonding-type interactions and thus to blocking of the original ICT that occurs in the polymers. Furthermore, upon complexation with H^+, both frontier orbitals (HOMO and LUMO) are located only over the polymer backbones. This cannot give a completely charge-separated state for an effective ICT process, and thus the fluorescence is enhanced for both **P1** and **P2** after their complexation with H^+. The anti-aromaticity of the acenaphthylene ring in **P3** makes it a less electron-rich center compared with the aromatic benzodithiophene (in **P1**) and phenanthrene (in **P2**) units. Thus, the HOMO electron cloud is not fully delocalized over the acenaphthylene unit in **P3**. The LUMO electron cloud is localized over the polymer backbone. Unlike in **P1** and **P2**, the charge-separated states are not well-defined in the case of **P3**. However, upon complexation with H^+ ions, a well-organized charge-separated state appears in **P3**. Finally, this causes an effective charge transfer in the polymer backbone. This can be attributed to the plausible quenching mechanism in **P3**.

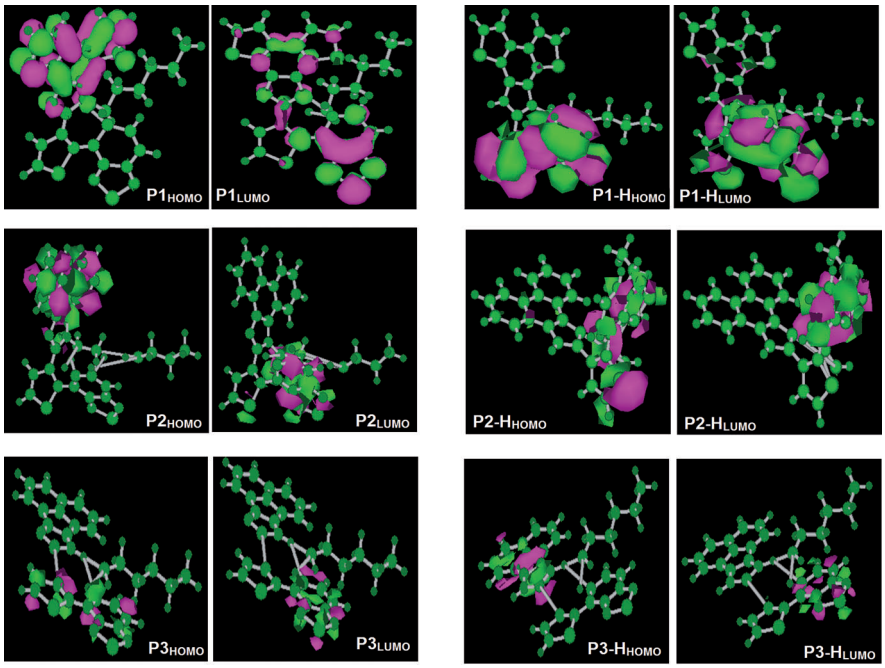

Figure 5. Localization of electron clouds in HOMO and LUMO of **P1**–**P3** before (left) and after (right) complexation with H^+.

presence of 10 equiv of Fe^{2+}. This may have been due to a better coordination ability of imidazole receptors towards Fe^{2+} ions, which may be attributed to energy- and/or charge-transfer due to the stronger ligand–metal interaction.[16e] The selectivity for Fe^{2+} was further proven by its interference with other background metal ions. As illustrated in Figure 7, the sensitivities of polymers **P1**–**P3** towards Fe^{2+} were not significantly affected by other competing metal ions. However, **P3** showed better quenching efficiency compared to those of **P1** and **P2**. This could be attributed to the higher molecular weight of **P3**, which gave rise to a better semiconducting "molecular wire effect" than **P1** and **P2**. The larger number of repeat units in **P3** provided more binding sites and thus caused complete fluorescence quenching.

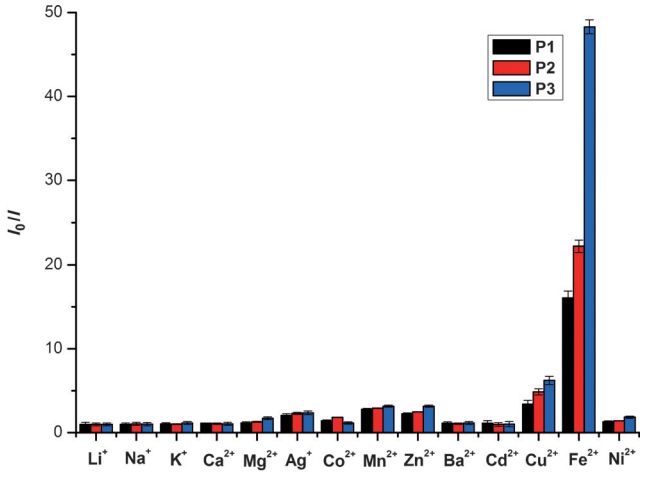

Figure 6. Fluorescence emission response profiles (I_0/I with error bars) of **P1**, **P2**, and **P3**. Polymer concentration (1.2×10^{-5} M), Fe^{2+} added = 10 equiv (1.2×10^{-4} M), other metal ions added = 30 equiv (3.6×10^{-4} M) (single-metal system).

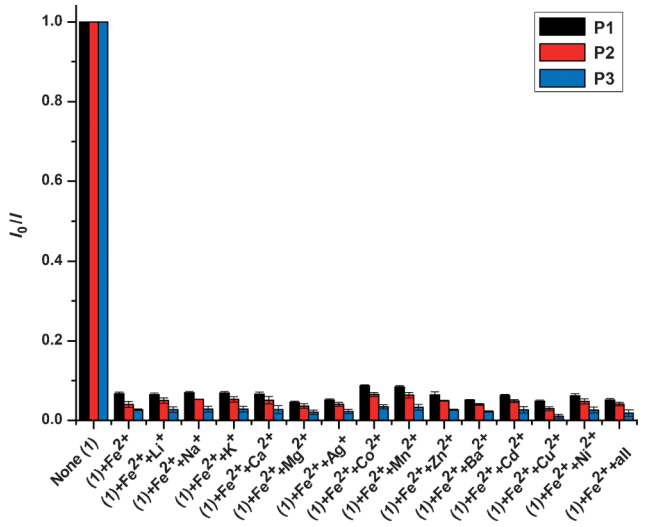

Figure 7. Fluorescence emission response profiles (I/I_0 with error bars) of **P1**, **P2**, and **P3**. Polymer concentration (1.2×10^{-5} M), $[Fe^{2+}] = 1.2\times10^{-4}$ M (10 equiv) and in the presence of other metal ions at 1.2×10^{-4} M (10 equiv) (dual-metal system).

Selectivity, sensitivity, and reversibility in metal ion sensing: The chemosensing properties of the fluorescent polymers were investigated for a variety of metal ions, such as Li^+, Na^+, K^+, Ca^{2+}, Ba^{2+}, Mg^{2+}, Zn^{2+}, Co^{2+}, Ni^{2+}, Cd^{2+}, Fe^{2+}, Ag^+, Mn^{2+}, and Cu^{2+} (Figure 6). The fluorescence intensities of **P1**–**P3** were only slightly altered upon the addition of up to 30 equiv of Li^+, Na^+, K^+, Ca^{2+}, Ba^{2+}, Ni^{2+}, Zn^{2+}, Ag^+, Co^{2+}, Mn^{2+}, and Cu^{2+}. However, the fluorescence intensities of polymers **P1**–**P3** were decreased significantly in the

The PL quenching efficiencies (PLQE) and static Stern–Volmer quenching constants (K_{SV}) are listed in Table 2. Due to the larger molecular wire effect, K_{SV} of **P3** is about 5.1 and 2.5 times higher than those of **P1** and **P2**, respectively. As depicted in Figure 8, sharp decreases in the fluorescence intensities of **P1**–**P3** were observed upon the addition of

Table 2. Photoluminescence quenching efficiency (PLQE) and Stern–Volmer quenching constants (K_{SV}) of polymers upon the addition of Fe^{2+}.

Metal Ion	Polymers	PLQE (%)[a]	K_{SV}[b]
Fe^{2+}	**P1**	78.22	2.01×10^{6}
	P2	81.57	4.12×10^{6}
	P3	96.94	1.03×10^{7}

[a] PLQE $=A_0-A/A_0$; where $A_0=$ area under the PL curve without metal ion, $A=$ area under the PL curve in presence of 10 equiv of metal ions. [b] Stern–Volmer quenching constants can be evaluated by the static Stern–Volmer equation $I_0/I=1+K_{SV}[Q]$, where I_0 is the PL intensity of the polymer (1.2×10^{-5} M) in the absence of the quencher, I is the PL intensity in the presence of each quencher, K_{SV} is the Stern–Volmer quenching constant, and [Q] is the quencher concentration.

Table 3. Photoluminescence properties of **P1**, **P2**, and **P3** upon titration with Fe^{2+}.

Sample	λ_{em}(nm)[a]	Φ_{em}[b]	τ[c]
P1	633	0.82	0.97
P1+Fe^{2+}	628	0.15	0.21
P2	640	0.84	1.12
P2+Fe^{2+}	632	0.11	0.18
P3	661	0.89	1.14
P3+Fe^{2+}	630	0.05	0.10

Fe^{2+} up to one molar equivalent. The fluorescence quantum yields and lifetimes of polymers **P1**–**P3** before and after the addition of Fe^{2+} are summarized in Table 3. Upon the addition of Fe^{2+}, the fluorescence lifetimes of the polymers decreased significantly (see Figure 9).[17] In the presence of Fe^{2+}, the fluorescence lifetimes of **P1** and **P2** were decreased almost 4.6- and 6.2-fold, respectively. The larger decrease in the fluorescence lifetime of polymer **P3** (11.4-fold) further confirmed its superior sensing ability due to its stronger molecular wire effect. Stern–Volmer plots for **P1**–**P3** in the presence of Fe^{2+} indicated 1:1 stoichiometries (Figure S1). Fluorescence recovery tests were carried out with two suitable counter ligands, namely the disodium salt of ethylenediaminetetraacetic acid (Na_2-EDTA) and phenanthroline. As illustrated in Figure 8, upon the addition of Na_2-EDTA or phenanthroline in THF to the quenched Fe^{2+}-polymer (**P1**–**P3**) solutions, the fluorescence intensities were about 65–85% recovered. This indicated the reversibility of the association of Fe^{2+} with imidazole units, and the preferential formation of a stable Fe-EDTA complex. Similarly, upon the addition of phenanthroline to the quenched Fe^{2+}-polymer (**P1**–**P3**) solutions, the fluorescence intensities were almost 90% recovered. This suggested that Fe^{2+} coordinates strongly through a double coordinating bond with phenanthroline, thereby releasing Fe^{2+} from the polymers. Thus, for the fully quenched Fe^{2+}-polymer (**P1**–**P3**) solutions, the phenanthroline-mediated fluorescence recovery was more prominent than that with EDTA. Photographs of the quenching and recovery of the fluorescences of each of the polymers (**P1**–**P3**) are also shown in the insets in Figure 8. Moreover, the fluorescence on-off-on behavior was observed over six successive cycles (Figure 10). Thus, a remarkable fluorescence on-off-on behavior was achieved for the polymer solutions for the sensing of Fe^{2+} based on reversible binding to the imidazole receptors and dissociation upon the addition of appropriate counter ligands (such as EDTA and phenanthroline) to form more stable complexes. To the best of our knowledge, this is the first report of intervention by the phenanthroline ligand eliciting efficient fluorescence recovery of imidazole receptors in the presence of metal ions.

To further elucidate the binding mode, ^{1}H NMR titrations were conducted by the addition of Fe^{2+} (in D_2O) to **M1**–**M3** (binding probes of **P1**–**P3**, respectively) in [D_8]THF (see Figure 11). In the case of **M1**, the signals of the aromatic protons were gradually shifted upfield upon the sequential addition of Fe^{2+}. The peak corresponding to the dibromothiophene unit was shifted upfield by 0.1 ppm (from $\delta=7.55$ to 7.45 ppm). Likewise, upon the addition of Fe^{2+}, a notable shift was observed in the signals of the aromatic protons corresponding to **M2**. That of the proton corresponding to dibromothiophene was shifted upfield by 0.13 ppm (from $\delta=$ 7.58 to 7.45 ppm). Unlike for **M1** and **M2**, the proton peak corresponding to the dibromothiophene unit in **M3** was dramatically downfield shifted. The signal of the dibromothiophene protons in **M3**, originally at $\delta=7.42$ ppm, was shifted downfield by 0.16 ppm to $\delta=7.58$ ppm. This was probably due to the different electronic distribution in **M3** due to the presence of the anti-aromatic acenaphthylene moiety (as discussed previously in relation to the computational analysis).

F^- sensing of 1-B, 2-B, 3-B, and 4-B: The precursors of monomers **M1**–**M4** (i.e., imidazole derivatives **1-B**, **2-B**, **3-B**, and **4-B** with free NH groups) were investigated for their halide ion sensing capabilities. As shown in Figure S2 (a)–(d), all of these imidazole derivatives were capable of sensing F^- effectively over other halides (Cl^-, Br^-, and I^-). Upon the addition of F^- to **1-B**, the PL peak at 500 nm decreased gradually (Figure S1(e)). Likewise, upon the addition of F^- (approaching 1 equiv) to **2-B**, the PL peak at 325 nm increased and a new peak simultaneously developed at 430 nm (Figure S1(f)). For **3-B**, the PL peaks at 325, 525, and 580 nm decreased upon the addition of F^- (Figure S1(g)). However, **4-B** showed the best sensing behavior towards F^- ions. The PL peak of **4-B** at 420 nm decreased gradually and a new peak developed at 504 nm with the addition of F^- (Figure S2(h)).

Conclusion

Three novel imidazole-based low-bandgap polymers (**P1**–**P3**) have been synthesized. Due to their donor–acceptor conjugations, these polymers show excellent photophysical and electrochemical properties (such as brilliant fluorescences, low bandgaps, large Stokes shifts, and low HOMO levels). As a result, they constitute structurally stable, semiconducting molecular wires capable of acting as promising

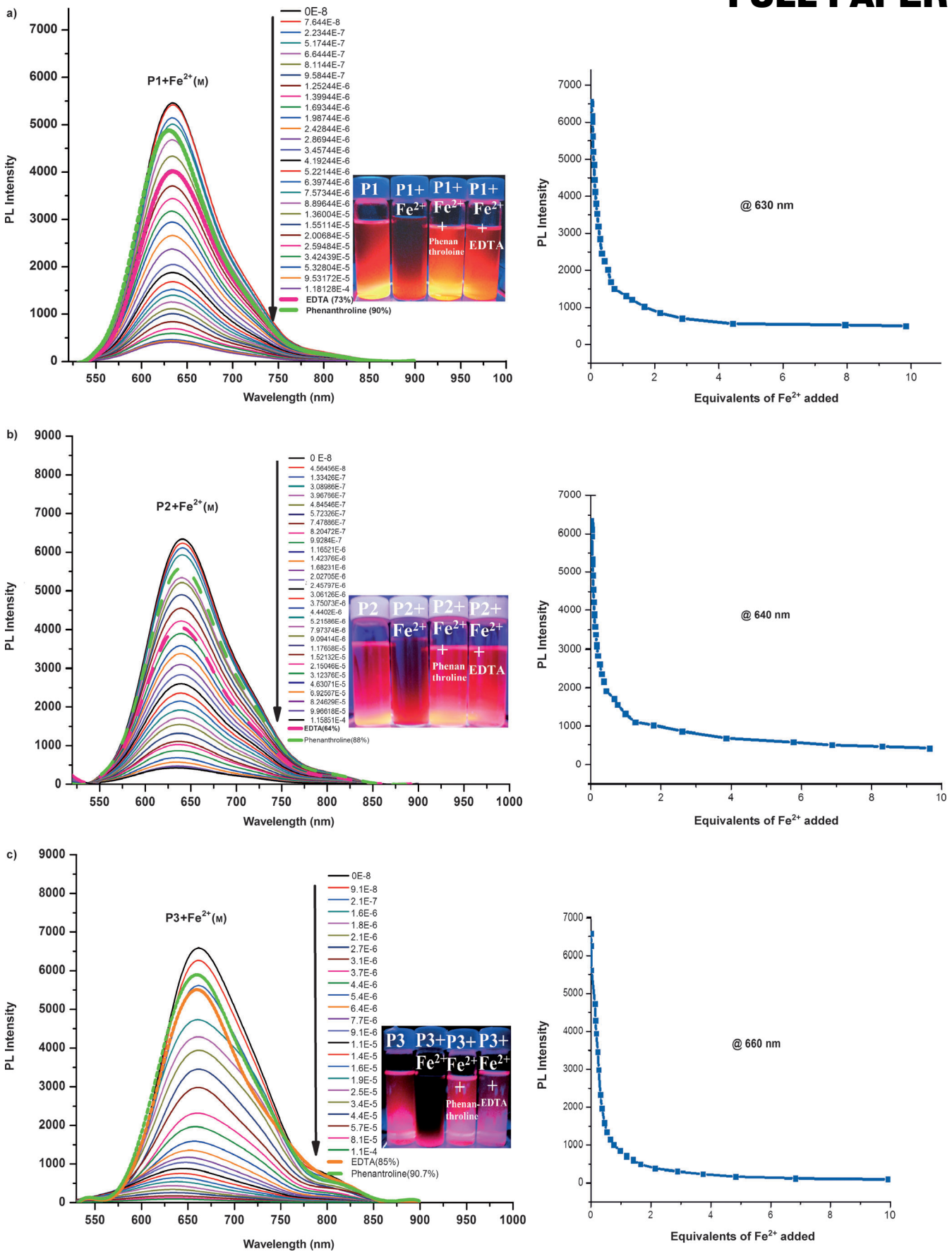

Figure 8. Sequential PL quenching of **P1** (a, left), **P2** (b, left), and **P3** (c, left) (1.2×10^{-5} M) in THF/H_2O (1:1) acquired by the addition of 0–10 equiv of Fe^{2+} and the recovery of fluorescence by the addition of Na_2-EDTA or phenanthroline. Lower insets: photographs of fluorescence quenching in the polymer solutions upon addition of Fe^{2+} and restoration of the original fluorescence upon addition of phenanthroline or Na_2-EDTA. PL quenching of **P1** (a, right), **P2** (b, right), and **P3** (c, right) as a function of 0–10 equiv [Fe^{2+}].

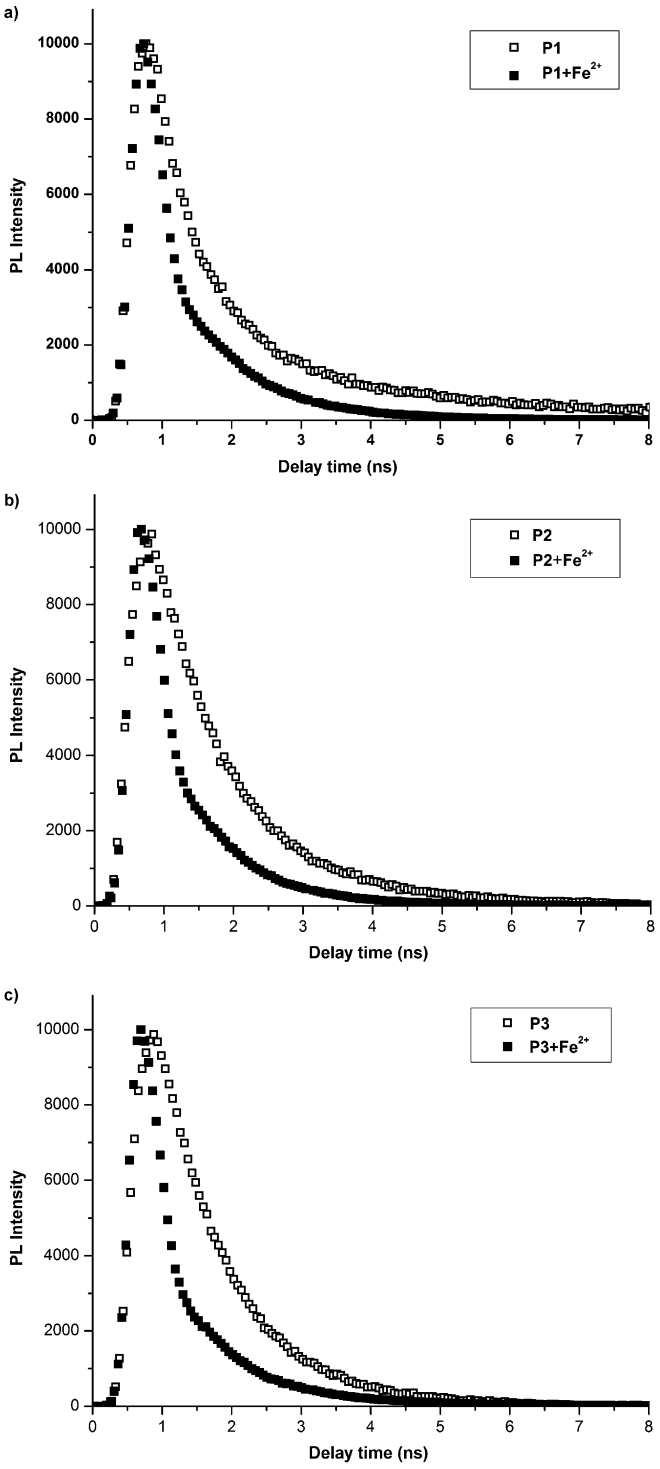

Figure 9. Time-resolved fluorescence of polymers **P1** (a), **P2** (b), and **P3** (c), before (empty circles) and after (solid circles) the addition of Fe^{2+}.

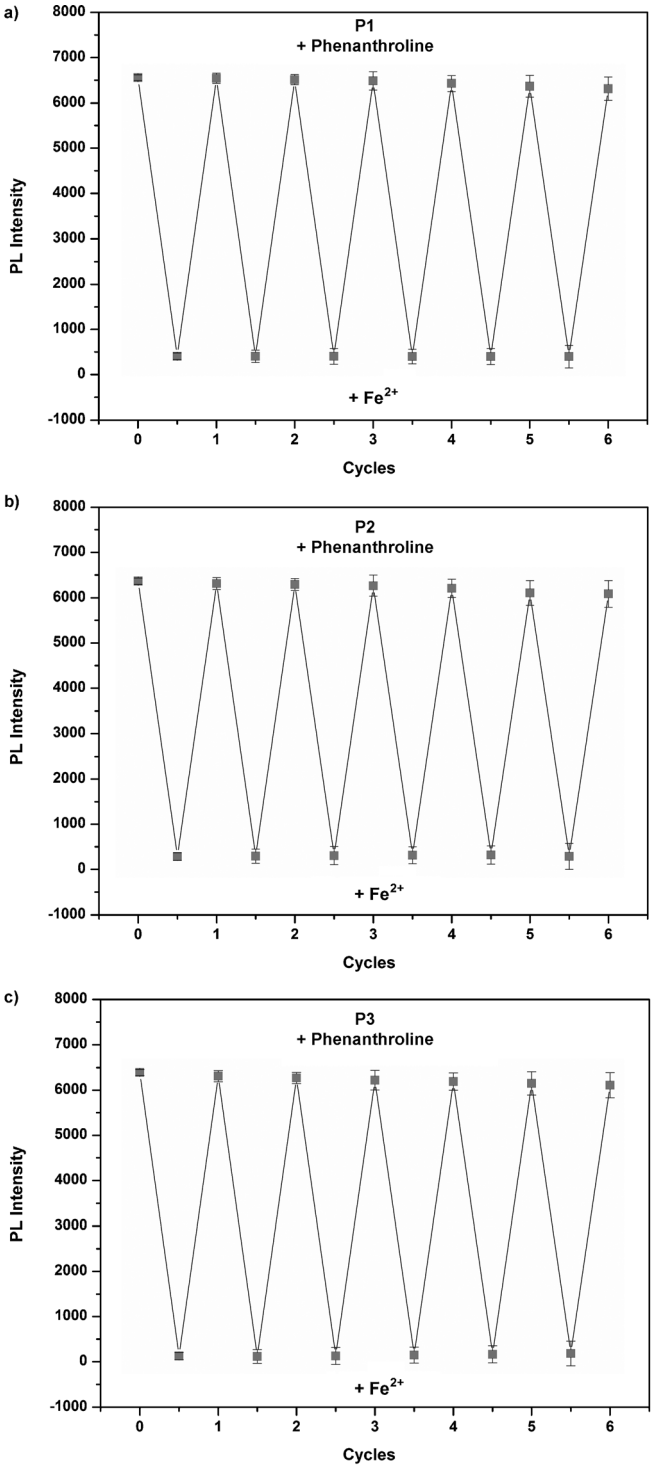

Figure 10. On-off-on switching of the fluorescence spectra of **P1** (a), **P2** (b), and **P3** (c,) over seven successive cycles (with error bars) upon the addition of Fe^{2+} and phenanthroline.

transduction materials for chemosensory applications. These imidazole-based polymers showed remarkable sensing capabilities towards H^+ and Fe^{2+} in semi-aqueous solutions. However, polymer **P3** showed a distinct sensitivity response compared with polymers **P1** and **P2**. Upon titration with H^+, polymer **P3** showed reduced absorption and fluorescence intensities due to static quenching. Polymers **P1** and **P2** showed hypsochromic shifts of their absorption and PL maxima, with enhanced fluorescence intensities under similar conditions. Compared with **P1** and **P2**, the anomalous behavior of **P3** was proven by computational analyses of the

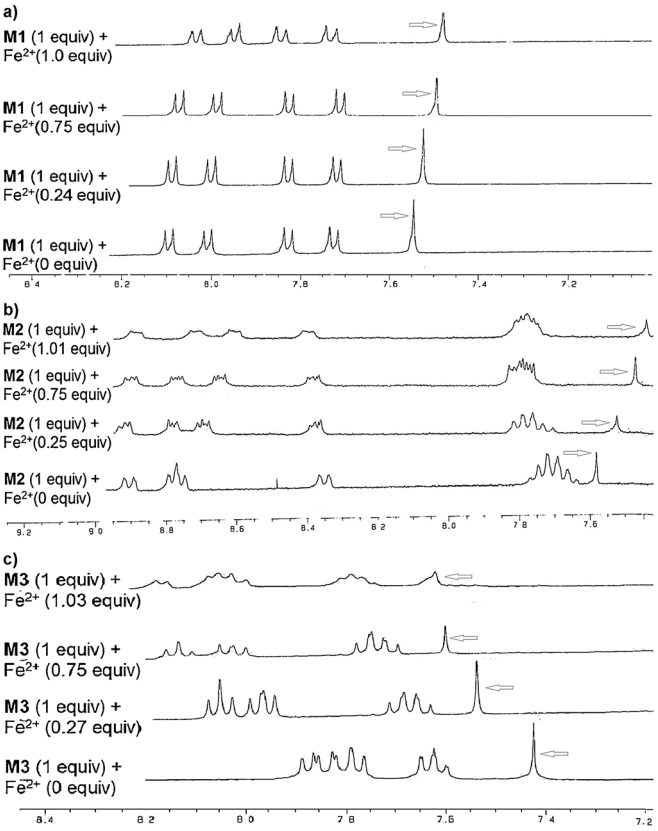

Figure 11. ^{1}H NMR titrations of monomers **M1** (a), **M2** (b), and **M3** (c) in [D_8]THF upon the sequential addition of 0–1 equiv of Fe^{2+} (in D_2O). (Arrow marks show the shifts of the peak corresponding to the dibromothiophene units).

electron densities in the HOMOs and LUMOs of **P1**–**P3** before and after complexation with H^+. Recoveries of the original fluorescences and absorptions were achieved by adding TEA. Furthermore, **P3** showed the best sensing ability for Fe^{2+} among **P1**–**P3** due to its stronger molecular wire effect. Correspondingly, in the presence of Fe^{2+}, the fluorescence lifetime of **P3** was extensively decreased (almost 11-fold) compared with those of polymers **P1** (4.6-fold) and **P2** (6.2-fold). ^{1}H NMR titrations with Fe^{2+} revealed distinct behavior of **P3** compared with **P1** and **P2**. The quenched fluorescences were recovered by adding Na_2-EDTA or phenanthroline. Thus, imidazole-based polymers can act as efficient chemosensing materials in terms of selectivity, sensitivity, and reversibility based on the on-off-on fluorescence protocol, which holds promise for future environmental and biological applications.

Experimental Section

Reagents: All chemicals and solvents were of reagent grade and were purchased from Acros, Aldrich, TCI, Fluka, TEDIA, or Lancaster Chemical Co. Toluene was dried by distillation over sodium/benzophenone before use. Chloroform ($CHCl_3$) and DMF were purified by refluxing with CaH_2 and then distilled. Solvents were degassed with nitrogen for 1 h prior to use when necessary.

Measurements and characterizations: ^{1}H and ^{13}C NMR spectra were recorded on a Bruker DX-300 spectrometer (300 MHz for ^{1}H, 75 MHz for ^{13}C) using $CDCl_3$ and [D_6]DMSO as solvents. Elemental analyses were performed on a HERAEUS CHN-OS RAPID elemental analyzer. Thermogravimetric analyses (TGA) were conducted with a TA Instrument Q500 at a heating rate of $10\,^\circ C\,min^{-1}$ under nitrogen. The molecular weights of the polymers were measured by gel permeation chromatography (GPC) using a Waters 1515 separation module, employing polystyrene standards, and eluting with tetrahydrofuran (THF). UV/Vis absorption spectra were recorded on an HP G1103A spectrophotometer from solutions in dilute solutions (10^{-5} M) in THF or as solid films (spin-coated on glass substrates from THF solutions with a concentration of $10\,mg\,mL^{-1}$). Cyclic voltammetry (CV) measurements were performed using a BAS 100 electrochemical analyzer with a standard three-electrode electrochemical cell in a 0.1 M solution of tetrabutylammonium hexafluorophosphate, (TBA)PF_6, in acetonitrile at room temperature at a scanning rate of $100\,mV\,s^{-1}$. Prior to the CV measurements, the solutions were purged with nitrogen for 30 s. In each case, a carbon working electrode coated with a thin layer of the polymer, a platinum wire as the counter electrode, and a silver wire as the quasi-reference electrode were used, and an Ag/AgCl (3 M KCl) electrode served as a reference electrode for all potentials quoted herein. The redox couple of ferrocene/ferrocenium ion (Fc/Fc^+) was used as an external standard. The corresponding HOMO and LUMO levels were calculated using $E_{ox/onset}$ and $E_{red/onset}$ from experiments on solid polymer films of similar thickness, which were deposited by drop-casting from solutions in chloroform (ca. $5\,mg\,mL^{-1}$). The onset potentials were determined from the intersections of two tangents drawn at the rising and background currents of the CV measurements. The pH-sensing properties were assessed in THF/H_2O (1:1) solutions by the addition of TFA as a proton source and TEA for reversibility tests. Similarly, the metal-sensing properties were assessed by the addition of metal ions to the polymer solutions in THF/H_2O (1:1). Reversibility in metal ion sensing was assessed using the disodium salt of ethylenediaminetetraacetic acid (Na_2-EDTA) or phenanthroline.

Acknowledgements

Financial support of this project has been provided by the National Science Council of Taiwan (ROC) through NSC 99–2113-M-009–006-MY2 and NSC 99–2221-E-009–008-MY2, and National Chiao Tung University through 97W807.

[1] a) J. D. Krooswyk, C. T. Tyrakowski, P. T. Snee, *J. Phys. Chem. C.* **2010**, *114*, 21348; b) R. A. Shimkunas, E. Robinson, R. Lam, S. Lu, X. Xu, X. Q. Zhang, H. Huang, E. Osawa, D. Ho, *Biomaterials* **2009**, *30*, 5720; c) L. Cui, Y. Zhong, W. Zhu, Y. Xu, Q. Du, X. Wang, X. Qian, Y. Xiao, *Org. Lett.* **2011**, *13*, 928; d) Y. Liu, C. Deng, L. Tang, A. Qin, R. Hu, J. Z. Sun, B. Z. Tang, *J. Am. Chem. Soc.* **2011**, *133*, 660; e) D. Maity, T. Govindaraju, *Chem. Commun.* **2010**, *46*, 4499; f) P. T. Snee, R. C. Somers, G. Nair, J. P. Zimmer, M. G. Bawendi, D. G. Nocera, *J. Am. Chem. Soc.* **2006**, *128*, 13320; g) Z. Q. Guo, W. H. Zhu, M. M. Zhu, X. M. Wu, H. Tian, *Chem. Eur. J.* **2010**, *16*, 14424; h) J. H. Jung, J. H. Lee, S. Shinkai, *Chem. Soc. Rev.* **2011**, *40*, 4464.

[2] a) T. Myochin, K. Kiyose, K. Hanaoka, H. Kojima, T. Terai, T. J. Nagano, *J. Am. Chem. Soc.* **2011**, *133*, 3401; b) F. Qian, C. Zhang, Y. Zhang, W. He, X. Gao, P. Hu, Z. Guo, *J. Am. Chem. Soc.* **2009**, *131*, 1460; c) D. Maity, T. Govindaraju, *Inorg. Chem.* **2010**, *49*, 7229; d) T. M. Swager, *Acc. Chem. Res.* **1998**, *31*, 201; e) R. Guliyev, A. Coskun, E. U. Akkaya, *J. Am. Chem. Soc.* **2009**, *131*, 9007; f) H. N. Kim, Z. Guo, W. Zhu, J. Yoon, H. Tian, *Chem. Soc. Rev.* **2011**, *40*, 79; g) M. Park, S. Seo, I. S. Lee, J. H. Jung, *Chem. Commun.* **2010**, *46*, 4478; h) D. Maity, A. K. Manna, D. Karthigeyan, T. K. Kundu, S. K. Pati, T. Govindaraju, *Chem. Eur. J.* **2011**, *17*, 11152; i) Z. Q. Guo, W. H. Zhu, H. Tian, *Macromolecules* **2010**, *43*, 739; j) D. Maity, T. Govindaraju, *Chem. Eur. J.* **2011**, *17*, 1410; k) H. Son, H. Y. Lee,

J. M. Lim, D. Kang, W. S. Han, S. S. Lee, J. H. Jung, *Chem. Eur. J.* **2010**, *16*, 11549; l) H. Y. Lee, D. R. Bae, J. C. Park, H. Song, W. S. Han, J. H. Jung, *Angew. Chem.* **2009**, *121*, 1265.

[3] a) F. S. Kim, G. Ren, S. A. Jenekhe, *Chem. Mater.* **2011**, *23*, 682; b) H. Usta, A. Facchetti, T. Marks, *Acc. Chem. Res.* **2011**, *44*, 501; c) A. C. Grimsdale, K. L. Chan, R. E. Martin, P. G. Jokisz, A. B. Holmes, *Chem. Rev.* **2009**, *109*, 897; d) L. Liao, A. Cirpan, Q. Chu, F. Karasz, Y. Pang, *J. Polym. Sci. Part A: Polym. Chem.* **2007**, *45*, 2048; e) Y. J. Cheng, S. H. Yang, C. S. Hsu, *Chem. Rev.* **2009**, *109*, 5868; f) M. Mas-Torrent, C. Rovira, *Chem. Rev.* **2011**, *111*, 4833; g) B. Y. Shao, X. Gong, A. J. Heeger, M. Liu, A. K. Y. Jen, *Adv. Mater.* **2009**, *21*, 1972; h) N. Cho, H. L. Yip, J. A. Davies, P. D. Kazarinoff, D. F. Zeigler, M. M. Durban, Y. Segawa, K. M. O'Malley, C. K. Luscombe, A. K. Y. Jen, *Adv. Eng. Mater.* **2011**, *1*, 1148; i) F. Huang, K. S. Chen, H. L. Yip, S. K. Hau, O. Acton, Y. Zhang, J. Luo, A. K. Y. Jen, *J. Am. Chem. Soc.* **2009**, *131*, 13886.

[4] a) D. T. McQuade, A. E. Pullen, T. M. Swager, *Chem. Rev.* **2000**, *100*, 2537; b) S. W. Thomas III, G. D. Joly, T. M. Swager, *Chem. Rev.* **2007**, *107*, 1339; c) B. Liu, H. Dai, Y. Bao, F. Du, J. Tian, R. Bai, *Polym. Chem.* **2011**, *2*, 1699; d) H. Lee, J. H. Lee, S. Kang, J. Y. Lee, G. John, J. H. Jung, *Chem. Commun.* **2011**, *47*, 2937; e) X. Duan, L. Liu, F. Feng, S. Wang, *Acc. Chem. Res.* **2010**, *43*, 260; f) H. Dong, X. Cao, C. Li, *ACS Appl. Mater. Interfaces* **2009**, *1*, 1599; g) X. Lou, Y. Zhang, J. Qin, Z. Li, *Chem. Eur. J.* **2011**, *17*, 9691; h) J. Li, Y. Wu, F. Song, G. Wei, Y. Cheng, C. Zhu, *J. Mater. Chem.* **2012**, *22*, 478.

[5] a) L. J. Fan, Y. Zhang, C. B. Murphy, S. E. Angell, M. F. L. Parker, B. R. Flynn Jr. , W. E. Jones, *Coord. Chem. Rev.* **2009**, *253*, 410; b) B. Liu, Y. Bao, H. Wang, F. Du, J. Tian, Q. Li, T. Wang, R. Bai, *J. Mater. Chem.* **2012**, *22*, 3555.

[6] a) S. W. Hong, C. H. Ahn, J. Huh, W. H. Jo, *Macromolecules* **2006**, *39*, 7694; b) Y. Clarke, W. Xu, J. N. Demas, B. A. DeGraff, *Anal. Chem.* **2000**, *72*, 3468; c) R. A. Potyrailo, *Angew. Chem.* **2006**, *118*, 718; *Angew. Chem. Int. Ed.* **2006**, *45*, 702; d) M. Kruppa, B. König, *Chem. Rev.* **2006**, *106*, 3520; e) O. A. Bozdemir, O. Buyukcakir, E. U. Akkaya, *Chem. Eur. J.* **2009**, *15*, 3830; f) A. Coskun, E. U. Akkaya, *J. Am. Chem. Soc.* **2006**, *128*, 14474; g) J. Jiang, X. Xiao, P. Zhao, H. Tian, *J. Polym. Sci. Part A: Polym. Chem.* **2010**, *48*, 1551.

[7] a) M. R. A. Blomberg, P. E. M. Siegbahn, M. Wikstrom, *Inorg. Chem.* **2003**, *42*, 5231; b) S. Yamamoto, H. Takeda, Y. Maki, O. Hayaishi, *J. Biol. Chem.* **1969**, *244*, 2951; c) G. E. Cartwright, C. J. Gubler, M. M. Wintrobe, *J. Biol. Chem.* **1957**, *224*, 533; d) M. Shellaiah, Y. C. Rajan, H C Lin, *J. Mater. Chem.* **2012**, *22*, 8976.

[8] a) P. Aisen, M. W. Resnick, E. A. Leibold, *Curr. Opin. Chem. Biol.* **1999**, *3*, 200; b) R. S. Eisenstein, *Annu. Rev. Nutr.* **2000**, *20*, 627; c) J. B. Neilands, *Ann. Rev. Biochem.* **1981**, *50*, 715; d) H. Ouchetto, M. Dias, R. Mornet, E. Lesuisse, J. M. Camadro, *Bioorg. Med. Chem.* **2005**, *13*, 1799; e) S. D. Kalinowski, C. P. Sharpe, V. P. Bernhardt, R. D. Richardson, *J. Med. Chem.* **2008**, *51*, 331; f) V. M. Chaud, C. Izumi, Z. Nahaal, T. D. Shuhama, L. P. M. Bianchi, O. Freitas, *J. Agric. Food Chem.* **2002**, *50*, 871; g) Q. Zou, X. Li, J. Zhang, J. Zhou, B. Sun, H. Tian, *Chem. Commun.* **2012**, *48*, 2095.

[9] a) J. B. S. Neilands, *Struct. Bonding (Berlin)* **1984**, *58*, 1; b) G. Winkelmann, D. van der Helm, J. B. Neilands, *Iron Transport in Microbes, Plants, Animals*, VCH Verlagsgesellschaft mbH, D-6940 Weinheim, Germany, **1987**; c) B. F. Matzanke, G. M. Matzanke, K. N. Raymond, *Iron Carriers, Iron Proteins*, VCH Publishers, New York, **1989**, 5; d) C. Brugnara, *Clin. Chem.* **2003**, *49*, 1573.

[10] a) S. Ghosh, C. K. Dey, R. Manna, *Tetrahedron Lett.* **2010**, *51*, 3177; b) Y. Liu, Q. Miao, S. W. Zhang, X. B. Huang, L. F. Zheng, Y. X. Cheng, *Macromol. Chem. Phys.* **2008**, *209*, 685; c) Q. Miao, X. B. Huang, Y. Q. Cheng, Y. Liu, L. L. Zeng, Y. X. Cheng, *J. Appl. Polym. Sci.* **2009**, *111*, 3137; d) X. Liu, X. Zhou, X. Shu, J. Zhu, *Macromolecules* **2009**, *42*, 7634; e) Y. Zhang, C. B. Murphy, W. E. Jones, *Macromolecules* **2002**, *35*, 630; f) A. R. Rabindranath, A. Maier, M. Schaer, B. Tieke, *Macromol. Chem. Phys.* **2009**, *210*, 659; g) M. Kimura, T. Horai, K. Hanabusa, H. Shirai, *Adv. Mater.* **1998**, *10*, 459; h) A. Maier, A. R. Rabindranath, T. Bernd, *Adv. Mater.* **2009**, *21*, 959; i) A. Maier, A. R. Rabindranath, B. Tieke, *Chem. Mater.* **2009**, *21*, 3668; j) S. J. Ou, Z. H. Lin, C. Y. Duan, H. T. Zhang, Z. P. Bai, *Chem. Commun.* **2006**, 4392; k) S. Watanabe, H. Seguchi, K. Yoshida, K. Kifune, T. Tadaki, H. Shiozaki, *Tetrahedron Lett.* **2005**, *46*, 8827; l) G. Saikia, P. K. Iyer, *Macromolecules* **2011**, *44*, 3753; m) A. K. Dwivedi, G. Saikia, P. K. Iyer, *J. Mater. Chem.* **2011**, *21*, 2502.

[11] a) A. P. Mykytiuk, D. S. Russell, R. E. Sturgeon, *Anal. Chem.* **1980**, *52*, 1281; b) A. A. Schilt, P. J. Taylor, *Anal. Chem.* **1970**, *42*, 220; c) D. Banerjea, K. Tripathi, *Anal. Chem.* **1960**, *32*, 1598; d) A. Safavi, H. Abdollahi, R. Mirzanjani, *Spectrochim. Acta Part A* **2006**, *63*, 196; e) A. Safavi, M. R. Hormozi Nezhad, *Can. J. Anal. Sci. Spectrosc.* **2004**, *49*, 210; f) A. M. Garcia Rodriguez, A. Garcia de Torres, J. M. Cono Pavon, C. Bosch Ojeda, *Talanta* **1998**, *47*, 463.

[12] a) S. Matuso, K. Kiyomiya, M. Kurebe, *Arch. Toxicol.* **1998**, *72*, 798; b) S.-W. Zhang, T. M. Swager, *J. Am. Chem. Soc.* **2003**, *125*, 3420; c) M. Laisalmi, H. Kokki, A. Soikkeli, H. Markkanen, A. Yli-Hankala, P. Rosenberg, L. Lindgren, *Acta Acad. Regiae Sci. Ups.* **2006**, *50*, 982; d) B. Liu, H. Tian, *J. Mater. Chem.* **2005**, *15*, 2681; e) W. Huang, Y. Li, Z. Yang, H. Lin, H. Lin, *Spectrochim. Acta Part A* **2011**, *79*, 471; f) O. B. Berryman, A. C. Sather, J. Rebek, *Org. Lett.* **2011**, *13*, 5232; g) H. Tong, L. Wang, X. Jing, F. Wang, *Macromolecules* **2003**, *36*, 2584; h) G. Zhou, Y. Cheng, L. Wang, X. Jing, F. Wang, *Macromolecules* **2005**, *38*, 2148; i) Y. Bao, B. Liu, H. Wang, J. Tian, R. Bai, *Chem. Commun.* **2011**, *47*, 3957; j) B. Chetia, P. K. Iyer, *Tetrahedron Lett.* **2008**, *49*, 94.

[13] a) A. S. Denisova, M. B. Degtyareva, E. M. Dem′yanchuk, A. A. Simanova, *Russian J. Org. Chem.* **2005**, *41*, 1690; b) C. M. Amb, P. M. Beaujuge, J. R. Reynolds, *Adv. Mater.* **2010**, *22*, 724.

[14] a) S.-H. Chan, C. P. Chen, T.-C. Chao, C. Ting, C. S. Lin, B. T. Ko, *Macromolecules* **2008**, *41*, 5519; b) I. H. Jung, J. Yu, E. Jeong, S. Kwon, H. Kong, K. Lee, H. Y. Woo, H. K. Shim, *Chem. Eur. J.* **2010**, *16*, 3743; c) C. P. Chen, S. H. Chan, T. C. Chao, C. Ting, B. T. Ko, *J. Am. Chem. Soc.* **2008**, *130*, 12828; d) Y. Xu, Y. Pang, *Chem. Commun.* **2010**, *46*, 4070; e) S. Atilgan, T. Ozdemir, E. U. Akkaya, *Org. Lett.* **2010**, *12*, 4792; f) P.-T. Wu, H. Xin, F. S. Kim, G. Ren, S. A. Jenekhe, *Macromolecules* **2009**, *42*, 8817; g) W. Yue, Y. Zhao, H. Tian, D. Song, Z. Xie, D. Yan, Y. Geng, F. Wang, *Macromolecules* **2009**, *42*, 6510; h) X. Liu, X. Shu, X. Zhou, X. Zhang, J. Zhu, *J. Phys. Chem. A.* **2010**, *114*, 13370.

[15] a) J. H. Huang, K. C. Li, D. Kekuda, H. H. Padhy, H. C. Lin, K. C. Ho, C. W. Chu, *J. Mater. Chem.* **2010**, *20*, 3295; b) N. Kleinhenz, L. Yang, H. Zhou, S. C. Price, W. You, *Macromolecules* **2011**, *44*, 872; c) Y. P. Zou, D. Gendron, R. Badrou-Aich, A. Najari, Y. Tao, M. Leclerc, *Macromolecules* **2009**, *42*, 2891.

[16] a) I. Valeur, B. Leray, *Coord. Chem. Rev.* **2000**, *205*, 3; b) M. Mameli, M. C. Aragoni, M. Arca, C. Caltagirone, F. Demartin, G. Farruggia, G. D. Filippo, F. A. Devillanova, A. Garau, F. Isaia, V. Lippolis, S. Murgia, L. Prodi, A. Pintus, N. Zaccheroni, *Chem. Eur. J.* **2010**, *16*, 919; c) A. P. De Silva, H. Q. N. Gunaratne, T. Gunnlaugsson, A. J. M. Huxley, C. P. McCoy, J. T. Rademacher, T. E. Rice, *Chem. Rev.* **1997**, *97*, 1515; d) L. Shen, X. Lu, H. Tian, W. Zhu, *Macromolecules* **2011**, *44*, 5612; e) S. M. Borisov, O. S. Wolfbeis, *Chem. Rev.* **2008**, *108*, 423; f) G. A. Hembury, V. V. Borovkov, Y. Inoue, *Chem. Rev.* **2008**, *108*, 1; g) Z. C. Xu, J. Yoon, D. R. Spring, *Chem. Soc. Rev.* **2010**, *39*, 1996.

[17] a) R. Satapathy, Y. H. Wu, H. C. Lin, *Chem. Commun.* **2012**, *48*, 5668; b) R. Satapathy, Y. H. Wu, H. C. Lin, *Org. Lett.* **2012**, *14*, 2564; c) P. J. Yang, H. C. Chu, T. C. Chen, H. C. Lin, *J. Mater. Chem.* **2012**, *22*, 12358; d) H. C. Chu, Y. H. Lee, S. J. Hsu, P. J. Yang, A. Yabushita, H. C. Lin, *J. Phys. Chem. B* **2011**, *115*, 8845.

Received: August 31, 2012
Revised: September 5, 2012
Published online: October 30, 2012

